

# Comparison of AFC and FACT Method for Periodic Disturbance Suppression in Optical Disk Drives

Jieng-Jang Liu\* Yee-Pien Yang†

Department of Mechanical Engineering, National Taiwan University, Taipei, Taiwan, R.O.C.

\* Email: jjliu@ntu.edu.tw

† Email: ypyang@ntu.edu.tw

**Abstract**—The adaptive frequency control (AFC) and frequency adaptive control technique (FACT) are effective methods in eliminating periodic disturbances. Especially for cancellation of repeatable runout in hard disk drives (HDD), AFC schemes have been applied successfully. This paper presents and compares the applicability from such two methods in optical disk drives (ODD). A surprising result is that a DC content dominating the periodic error signals is necessary for AFC schemes to function properly. This implies that AFC is inapplicable in systems where the DC content is small or intended to be reduced. The property is analytically examined through the well-known amplitude modulation (AM) process and is verified experimentally on the disk wobble compensation in ODD. Experimental results show that FACT has better properties than AFC in terms of DC reduction and harmonic independence. It is also shown that AFC fails if the DC content and harmonics are compensated simultaneously. Regarding the application on ODD, the FACT scheme is practical in disk runout and wobble control.

## I. INTRODUCTION

In rotating machinery, periodic disturbances are unavoidable. For data storage devices, such as hard disk drives (HDD) and optical disk drives (ODD), periodic disturbances appear in the error of position of the head or laser spot following the data track. In ODD, the track-following and focusing controls attempt to maintain the position of the laser spot over the target track in radial and vertical directions, respectively. Primarily, the repeatable runout in the position of the laser spot with respect to the center of track can be referred to as tracking errors in the track-following system. Similarly, the repeatable wobble in the position with respect to surface of the disk are referred to as focusing errors in focusing control. Although the well designed feedback controllers are adequate to satisfy most specifications, they do not have good tracking or focusing capabilities in the presence of periodic disturbances due to repeatable disk runout or wobble effects.

To achieve perfect regulation in the presence of disk runout, the AFC schemes were successfully used in HDD by way of feedforward control, which minimizes the magnitude of the error signals [1]-[5]. The design method of such algorithms was presented by Messner [6]. Recently, the FACT method has been developed to reduce the tracking error on ODD application [7]-[8]. This method considers the fact that the running speed and mode of disk are diverse in ODD, whereas those are unchangeable in HDD. Both AFC and FACT methods learn the true shape of the track to be followed on-line and output the inverse of the periodic disturbances to achieve high-accuracy regulation.

In principle, methods for reducing errors in track-following systems are capable of decreasing the focus-

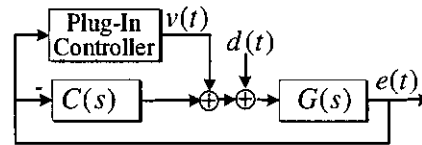


Fig. 1. The plug-in wobble reduction controller

ing errors in focusing control because their control strategies are implemented same as the standard feedback control. In fact, not only the periodic disturbances but also the DC component are encompassed in both the tracking and focusing errors on ODD. The DC value in tracking error comes from the steady-state deviation of radial position of lens with respect to the center of pick-up head (PUH) and acts as the source to actuate the sled motor movement of the dual-actuator setup in ODD. On the other hand, the DC content of focusing error results from the vertical displacement of lens from the free position to the focusing point and makes a significant contribution in focusing errors. Although the AFC schemes were devoted to the systems perturbed by periodic disturbances, the issues regarding the DC contribution have not been addressed.

In this paper, the AFC and FACT controllers, which are used in evaluating the viability of periodic disturbances reduction, are reviewed in respect of DC content reduction for focusing servo system on ODD. Both controllers are designed and installed as a plug-in module in the existing focusing servo system. It is shown that the AFC method is unable to reduce any harmonic if the DC content is not the dominator of the periodic focusing errors. By contrast, the FACT method is capable of reducing the periodic disturbances and DC content simultaneously.

## II. THE FEEDFORWARD COMPENSATION

The plug-in feedforward adaptive controller, as shown in Fig. 1, was designed to minimize the focus error signals (FES) of the focus servo system in ODD. The plant  $G(s)$  contaminated by the disturbance  $d(t)$  is controlled by the feedback controller  $C(s)$  as well as the compensation  $v(t)$  through the plug-in controller, wherein  $C(s)$  is designed so that the feedback system is stable. The DC component of  $d(t)$  causes the plant output  $e(t)$  to have a corresponding constant steady state error, while the sinusoidal disturbances cause  $e(t)$  to have significant excitation of harmonics. Assume that the transfer function from  $v(t)$  to  $e(t)$  is expressed as

$$\frac{E(s)}{V(s)} = \frac{G(s)}{1 + G(s)C(s)} \triangleq W(s). \quad (1)$$

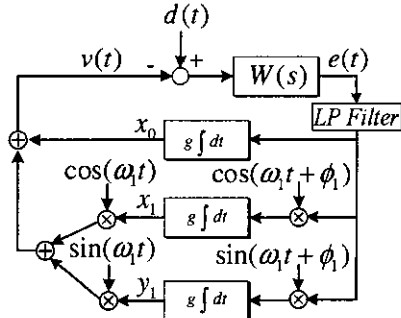


Fig. 2. Generalized AFC architecture.

The adaptive signal  $v(t)$  is designed so that the sinusoidal excitations on  $e(t)$  are reduced by injecting the additive inverse to the input of the plant. That is, if  $e(t)$  is composed of  $M$  order of sinusoidal functions,  $v(t)$  is defined as

$$v(t) = \sum_{n=0}^M v_n(t) = \sum_{n=0}^M (x_n \cos \omega_n t + y_n \sin \omega_n t) \quad (2)$$

where  $x_n$  and  $y_n$ , denoting as on-line adaptive variables, are formulated according to the adaptive rules of AFC and FACT schemes.

### III. GENERALIZED AFC SCHEME

Developed by Bodson [1], the AFC algorithm is employed to reduce undesired harmonics. A generalized algorithm of AFC is proposed in Fig. 2, where the disturbance  $d(t)$  includes not only the sinusoidal contents but also a DC component. Contrast to the basic AFC algorithm, the current algorithm employs a low-pass filter so that the valuable low frequency contents of  $e(t)$  can be preserved while the high frequency noises can be suppressed. To simplify the notation without loss of generality, it is assumed that  $d(t)$  is composed of a DC component and the fundamental frequency, i.e.,

$$d(t) = a_0 + a_1 \cos(\omega_1 t) + b_1 \sin(\omega_1 t) \quad (3)$$

where  $a_0$ ,  $a_1$ , and  $b_1$  are unknown constants. In cases that there are many harmonics to be compensated, the extensions are straightforward. According to (2), the control  $v(t)$  is selected to be

$$v(t) = x_0 + x_1 \cos(\omega_1 t) + y_1 \sin(\omega_1 t) \quad (4)$$

so that the disturbance is exactly compensated when the on-line adaptive variables have nominal values

$$x_0^* = a_0, \quad x_1^* = a_1 \text{ and } y_1^* = b_1 \quad (5)$$

Letting that  $\phi_1 = \angle W(j\omega_1)$  and

$$\theta = \begin{bmatrix} x_0 \\ x_1 \\ y_1 \end{bmatrix}, w = \begin{bmatrix} 1 \\ \cos(\omega_1 t + \phi_1) \\ \sin(\omega_1 t + \phi_1) \end{bmatrix}, \theta^* = \begin{bmatrix} a_0 \\ a_1 \\ b_1 \end{bmatrix} \quad (6)$$

the output  $e(t)$  can be written as

$$e = W[(\theta - \theta^*)^T w] \quad (7)$$

where  $W$  is defined in (1), then a possible update law for the on-line adaptive variables is

$$\dot{x}_0(t) = g_0 e(t) \quad (8)$$

$$\dot{x}_1(t) = g_1 e(t) \cos(\omega_1 t + \phi_1) \quad (9)$$

$$\dot{y}_1(t) = g_1 e(t) \sin(\omega_1 t + \phi_1) \quad (10)$$

where the parameters  $g_0$  and  $g_1$  refer to as the adaptation gains. If  $W(s)$  is stable and  $\text{Re}[W(j\omega_1)] > 0$ , the adaptive algorithm is convergent and  $e(t)$  tends towards zero by choosing a sufficiently small adaptation gains. It was shown by Bayard [9] that an AFC system can be expressed as an exact linear time-invariant (LTI) representation. The corresponding LTI relationship between the Laplace transform of the input,  $e(t)$ , and that of the output,  $v(t)$ , in Fig. 2 is

$$\frac{V(s)}{E(s)} = g_0 \frac{\cos(\phi_1)}{s} + g_1 \frac{\cos(\phi_1)s + \sin(\phi_1)\omega_1}{s^2 + \omega_1^2} \quad (11)$$

It is clear that there exists a pair of complex conjugate poles at  $s = \pm j\omega_1$  and a single pole at  $s = 0$ . According to the internal model principle [10], the equivalent controller includes the disturbance generation elements by which the disturbance can be reduced.

If  $e(t)$  is sampled at a rate of  $N$  samples per revolution of disk, the adaptation algorithms in (8)-(10) are most likely to be implemented as the following discrete-time versions:

$$x_0(k+1) = x_0(k) + g_0 e(k) \quad (12)$$

$$x_1(k+1) = x_1(k) + g_1 e(k) \cos(\omega_1 k + \phi_1) \quad (13)$$

$$y_1(k+1) = y_1(k) + g_1 e(k) \sin(\omega_1 k + \phi_1) \quad (14)$$

with the corresponding control law as

$$v(k) = x_0(k) + x_1(k) \cos(\omega_1 k) + y_1(k) \sin(\omega_1 k) \quad (15)$$

In case that the disk has speed of  $\omega_1$  revolutions per second and the  $M$  order of sinusoidal components are to be reduced, the highest frequency component in  $e(t)$  is now of  $M\omega_1$  Hz. Thus, for a desirable stability, the least value of  $N$  can be given in terms of  $M$  and  $\omega_1$ , as follows:

$$N\omega_1 > 2M\omega_1 \quad (16)$$

which yields

$$N > 2M. \quad (17)$$

Making the  $N$  larger tends to make the discrete-time version behave more like the continuous-time system. It is important to point out that the equally spaced points  $N$  is determined by  $M$  alone and is independent of  $\omega_1$ . This implies that even the speed or the running mode is changed, the  $M$  harmonics can be reduced all the time. For basic AFC without a low-pass filter in series, the adaptive rate is specified the same as the sampling rate of the overall discrete-time system; and consequently, it can be implemented in the case where the disk has a unique running speed.

#### A. Amplitude Modulation Property in AFC

For LTI system  $W(s)$  in Fig. 2, the plant output  $e(t)$ , having the same form as the input  $d(t)$ , can be represented as

$$e(t) = \bar{a}_0 + \bar{a}_1 \cos(\omega_1 t) + \bar{b}_1 \sin(\omega_1 t) \quad (18)$$

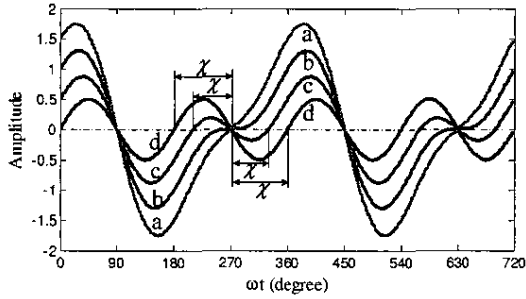


Fig. 3. The amplitude of the right hand side of (21) with  $\hat{a} = 1$ ,  $\hat{b} = 0$  and various  $\bar{a}_0$ . The lines indicate as a, b, c, d corresponding to the cases that  $\bar{a}_0$  has value of 1.5, 1, 0.5, and 0, respectively. When  $\bar{a}_0 < \hat{a}$ , the regions labeled by  $\chi$  on lines c and d have opposite values on those of lines a and b.

where  $\bar{a}_0$ ,  $\bar{a}_1$ , and  $\bar{b}_1$  are unknown constants because  $a_0$ ,  $a_1$ , and  $b_1$  in (3) are previously unknown. Using (18), the right-hand side of (9) gives

$$\begin{aligned}
 & g_1 e(t) \cos(\omega_1 t + \phi_1) \\
 &= g_1 (\bar{a}_0 + \bar{a}_1 \cos(\omega_1 t) + \bar{b}_1 \sin(\omega_1 t)) \cos(\omega_1 t + \phi_1) \\
 &= g_1 \bar{a}_0 \cos(\omega_1 t + \phi_1) \\
 &\quad + g_1 (\bar{a}_1 \cos(\omega_1 t) + \bar{b}_1 \sin(\omega_1 t)) \cos(\omega_1 t + \phi_1) \\
 &= g_1 \bar{a}_0 \cos(\omega_1 t + \phi_1) \\
 &\quad + g_1 (\hat{a} \sin(\omega_1 t + \hat{b})) \cos(\omega_1 t + \phi_1), \quad (19)
 \end{aligned}$$

where  $\hat{a}$  and  $\hat{b}$  are related to  $\bar{a}_1$  and  $\bar{b}_1$  as

$$\hat{a} \sin(\omega_1 t + \hat{b}) = \bar{a}_1 \cos(\omega_1 t) + \bar{b}_1 \sin(\omega_1 t). \quad (20)$$

If the constant gain  $g_1$  and relative phase  $\phi_1$  in (19) are ignored, there results

$$\begin{aligned}
 e(t) \cos(\omega_1 t) &= \bar{a}_0 \cos(\omega_1 t) + \hat{a} \sin(\omega_1 t + \hat{b}) \cos(\omega_1 t) \\
 &= \mathbb{A} + \mathbb{B} \quad (21)
 \end{aligned}$$

showing that portion  $\mathbb{A}$  is the unmodulated carrier of level  $\bar{a}_0$  and portion  $\mathbb{B}$  is the modulation product. The operation is similar to a system known as amplitude modulation (AM) [11], where the carrier signal  $\cos(\omega_1 t)$  is modulated by means of a signal of  $\sin(\omega_1 t + \hat{b})$ . The important facts are that in (21) the frequency of carrier signal is the same as that of modulating signal and that the portions  $\mathbb{A}$  and  $\mathbb{B}$  are in phase with each other only if the condition  $\bar{a}_0 \geq \hat{a}$  is satisfied. That is, the sign of modulated output not only depends on the angle of  $\omega_1 t$  but also the amplitudes of  $\bar{a}_0$  and  $\hat{a}$ . In terms of the terminology in AM processing, the condition of  $\bar{a}_0 = \hat{a}$  refers to as full modulation and distortion occurs if  $\bar{a}_0 < \hat{a}$ . Such phenomenon can be illustrated by a simple graph as follows. For example, without loss the generality, letting  $\hat{a} = 1$  and  $\hat{b} = 0$ , Fig. 3 demonstrates the values of (21) in cases that the  $\bar{a}_0$  varies in some values such as 1.5, 1, 0.5, and 0. It is seen that the regions labeled by  $\chi$  on lines c and d have values that are opposite to those in lines of a and b, which is the result that the distortion occurs when  $\bar{a}_0 < \hat{a}$ . The reverse sign makes an incorrect adaptation gain which in turn results in a failure adaptation. Consequently, the amplitude of the DC component larger than that of other harmonics is an essential requirement for the modulation to take place faithfully. This

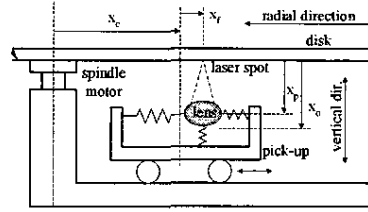


Fig. 4. Optical disk mechanism.

implies that a dominant DC content in  $e(t)$  is necessary for the AFC algorithm to function successfully. It can be concluded that the DC content and any harmonic cannot be compensated simultaneously by AFC method.

### B. Intrinsic Nature of DC Component

For data storage devices used in the computer, such as HDD and ODD, the available power sources are unipolar, that is, +12 and +5 volts. The zero crossing point is shifted by a constant level, for example, +1.85 volt for the experimental drive in this paper, so that the internal signals behave as bipolar, which is needed in servo configuration. In this way, there is always a DC content involved in FES of focusing system. Without pruning away the shifting constant or the true FES having amplitude in sizable value, the harmonic components can be reduced by AFC method. The applications in HDD to reduce the runout effects are classified into this group [3], [5], [12]. For the ODD used in this paper, however, the maximum allowable FES is limited in  $\pm 1 \mu\text{m}$ , which is equivalent to a voltage variation of  $\pm 63 \text{mV}$ . Compared with the shifting constant, the true FES is insignificant even at the worst condition. Involving with shifting constant, the mathematical operations are inefficient and additional bits of data words are needed to realize the data processing. To make a practical data processing, the shifting constant must be removed.

## IV. THE FOCUS SERVO SYSTEM IN ODD

Figure 4 illustrates the schematic setup of a typical ODD system. The mechanism is composed of a spindle motor for the rotation of the disk, an optical PUH for focusing and track following, and a coarse actuator to move the pick-up assembly in radial direction. The focusing system directs the movement of the lens in vertical direction and maintains the laser spot on the disk within its suitable range of focus. Since the free position  $x_o$ , as depicted in Fig. 4, cannot guarantee to be a suitable position to initiate the focusing action, a search process detects the focus point  $x_p$  and then turns on the focusing servo so that the focus point can be locked.

One important character is that the free position  $x_o$  always differs from that of focusing point  $x_p$  when the focusing system functions properly. This implies that there exists a constant bias force to pull the lens to the free position  $x_o$  constantly. Since the displacement  $|x_p - x_o|$  differs if the drive or disk is replaced, the bias force varies accordingly. Hence, the FES always contains a significant DC content due to this external bias force. It is of most significant that the DC component is likely to dominate FES depending on the disk speed and physical properties of

TABLE 1  
THE IDENTIFIED PARAMETERS OF  $W(s)$ .

CAV 4,500 rpm				CAV 6,780 rpm			
Hz	$W_r(\omega_n)$	$W_i(\omega_n)$	$\phi_n$	Hz	$W_r(\omega_n)$	$W_i(\omega_n)$	$\phi_n$
0	0.8410	0	0°	0	0.8410	0	0°
75	0.8726	0.0704	4.6°	113	0.9111	0.1190	8.1°
150	0.9658	0.1207	7.1°	226	1.1166	0.1771	9.0°
225	1.1158	0.1300	6.6°	339	1.4426	0.1037	0.1°
300	1.3143	0.0759	3.3°	452	1.8490	-0.1993	-6.1°
375	1.5474	-0.067	-2.5°	565	2.2057	-0.8764	-21.6°

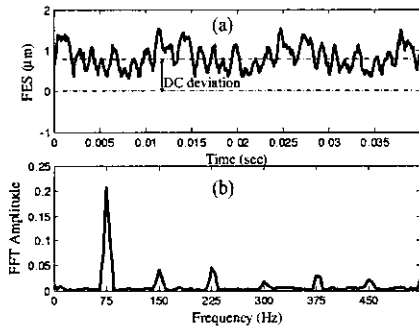


Fig. 5. The time series and FFT spectrum of FES at 4,500rpm (75Hz) without the help of AFC or FACT compensation.

disk. Furthermore, a slant turntable causes such DC content to vary slowly when the PUH moves within the entire radial range.

#### V. EXPERIMENTAL IMPLEMENTATION AND RESULTS

The experimental setup for implementation consists of a commercial high-speed CD-ROM drive and a field programmable gate array (FPGA) device. In addition to controller  $C(s)$ , the AFC, FACT and additional interfacing signals are implemented digitally into the single FPGA chip.

With a properly designed feedback controller  $C(s)$ , the frequency response  $W(s)$  defined in (1) can be identified and the parameters needed to implement the AFC and FACT are illustrated in Table 1. In the experiment results shown below, both the AFC and FACT methods are designed to compensate the first five harmonics of FES. For a standard test disk with  $1 \pm 0.05mm$  in vertical deviation [13], Fig. 5 shows the time series and FFT spectrum of FES at CAV 4,500rpm. It is seen that the DC deviation and harmonics are significant. The positive DC content indicates that the lens has a constant downward deviation from the focusing point. The DC content dominates the FES energy in the present case.

##### A. Verification of AM Property in AFC

As stated previously, a dominant DC component is necessary for the AFC algorithm to be realized. If the DC content is reduced out or is not dominant in the FES, the AFC fails because distortion occurs from the AM processing. To show this feature, Fig. 6 represents a series of actions when both the fundamental harmonic and DC content are to be reduced, in which the DC content is reduced by fraction of 25%, 50%, and 75%, respectively. It is clear that the more the fraction of DC content is reduced, the closer the

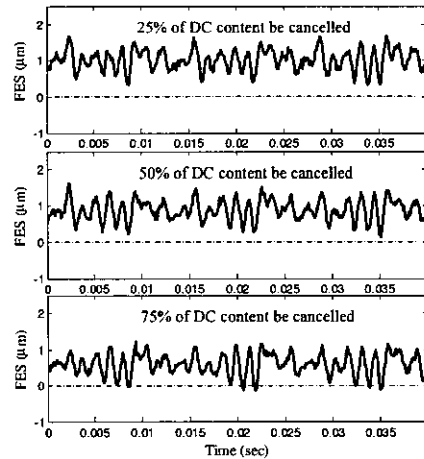


Fig. 6. The AFC results when both the fundamental and fractional DC contents are reduced.

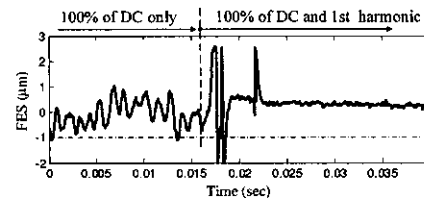


Fig. 7. 100% of DC reduction followed by an additional 1st harmonic compensation causes the FES out of control.

FES trajectory is to the zero line. However, it is impossible for the AFC to have both the fundamental and 100% of DC contents reduced concurrently, as shown in Fig. 7 where the FES becomes uncontrollable and the focusing servo turns off. The results verify the discussion in Section III-A.

##### B. DC and Harmonic Reduction in FACT

Contrast to the AFC method, the FACT provides a superior selection to deal with the condition when both the harmonics and DC content are to be reduced simultaneously. In fact, with respect to the FACT method, the contents in FES are decoupled independently. Therefore, a 100% DC content together with any harmonics can be reduced at the same time. For example, both the 100% DC and fundamental contents are reduced concurrently in Fig. 8.

In the case that the disk is running at a higher speed, for example CAV 6,780rpm (113Hz), Fig. 9 shows the corresponding FES if the feedback controller  $C(s)$  is the same as that used in CAV 4,500rpm. As expected, the controller  $C(s)$ , which is not designed for this current speed, provides inadequate open-loop gain at wobble frequencies. Instead of the DC content, the fundamental harmonic dominates

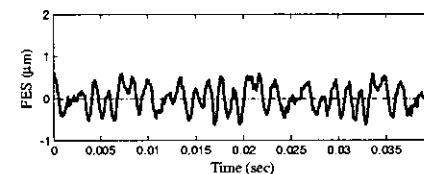


Fig. 8. By FACT method, both the fundamental frequency and 100% DC contents can be reduced concurrently.

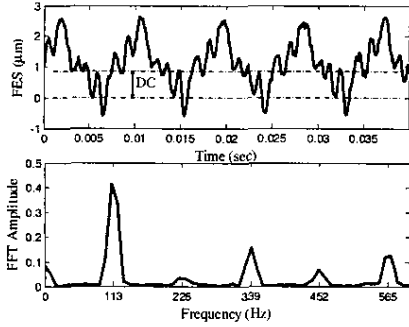


Fig. 9. The time series and FFT spectrum of FES at 6.780 rpm (113Hz) without the help of AFC or FACT.

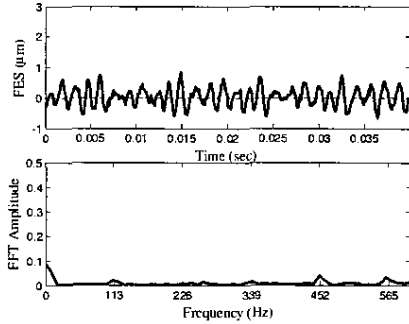


Fig. 10. With the help of FACT, the DC and the five harmonics are reduced successfully for CAV 6, 780rpm.

the energy in FES, which has a maximum amplitude up to  $2.5\mu m$ . In this condition, the AFC method cannot be applied because the AM process fails. By FACT, however, the DC content as well as the five harmonics can be reduced successfully, as shown in Fig. 10. It is seen that the FES satisfies the specification in  $\pm 1\mu m$  dramatically.

### C. Experiment on the CLV mode

In addition to the CAV mode for high speed operation, the slow speed CLV mode also plays important roles in ODD's. The harmonic effects are insignificant due to the slow running speed. However, it is helpful to compensate the DC content and the fundamental harmonic. For example, Fig. 11 shows the trajectory of FES at CLV-6x speed without the help of AFC or FACT. Obviously, a notable DC deviation and fundamental frequency excitation are observed. It is

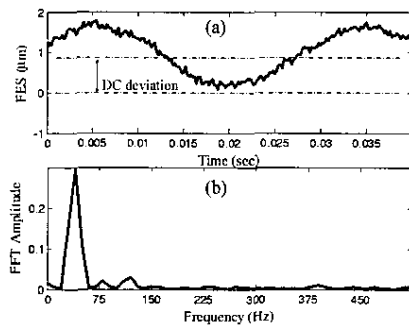


Fig. 11. The time series and FFT spectrum of FES at CLV-6x without the help of AFC or FACT compensation.

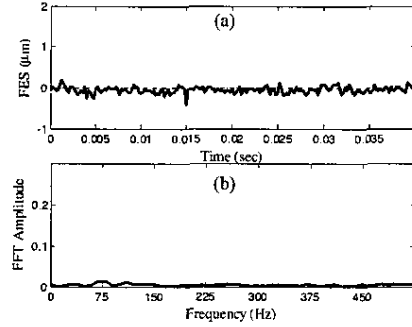


Fig. 12. With the help of FACT, the DC and the fundamental contents are reduced successfully at CLV-6x.

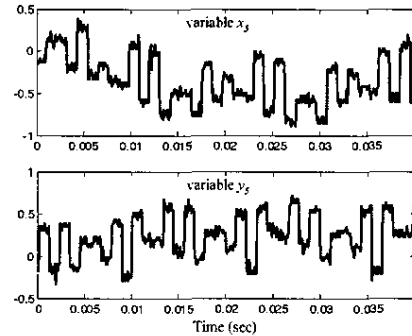


Fig. 13. The trajectories of adaptive variables  $x_5$  and  $y_5$  when the AFC was applied at time zero.

clear that the AFC method will not work in this case but the FACT will as shown in Fig. 12.

### VI. CONVERGENT PROPERTY OF AFC AND FACT

The convergent property for variables  $x_n$  and  $y_n$  in (2) reveals the essential difference between AFC and FACT methods. As shown in (8)-(10), the variables  $x_n$  and  $y_n$  governed by AFC rely on the sampled value of  $e(t)$ . If  $e(t)$  includes  $M$  order harmonics, all harmonics are coupled concurrently to generate  $x_n$  and  $y_n$ . As a result, the output  $v_n(t)$  for the  $n$ th harmonic in (2) will be contaminated by other harmonics. For example, Fig. 13 depicts the trajectories of  $x_5$  and  $y_5$  when the AFC method was applied at CAV 4,500rpm. The corresponding output  $v_5$  shown in Fig. 14 indicates that  $v_5$  is not a pure sinusoidal function at

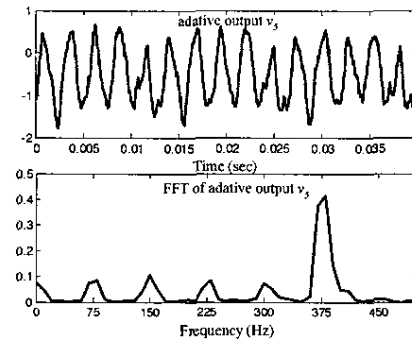


Fig. 14. The adaptive output  $v_5$  as the  $x_5$  and  $y_5$  are depicted in Fig. 13.

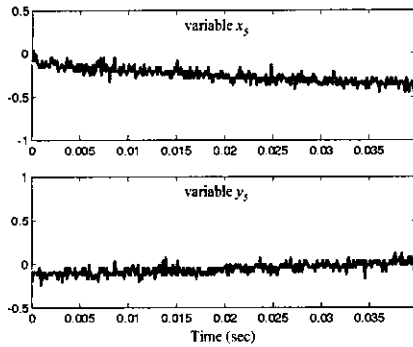


Fig. 15. The trajectories of adaptive variables  $x_5$  and  $y_5$  when the FACT was applied at time zero.

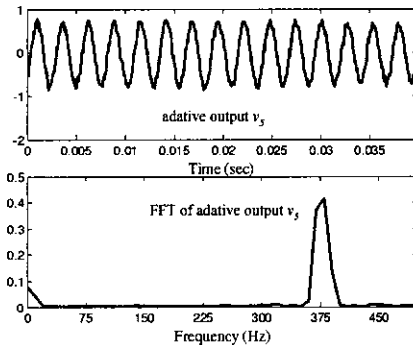


Fig. 16. The adaptive output  $v_5$  if the  $x_5$  and  $y_5$  are depicted in Fig. 15.

375Hz but includes components at 75Hz, 150Hz, 225Hz and 300Hz. Depending on the phase of these components, FES could be either reduced or enlarged at these frequencies when the fifth harmonic was reduced by AFC method. The outcome discussed here also provides an alternative interpretation of the harmonic generation effect introduced by Bodson [1].

By FACT, however, the consequences are much different. Figure 15 shows that the variables  $x_5$  and  $y_5$  converge toward constant values because each harmonic is independently determined. Accordingly, the output  $v_5$  behaves as a perfect fifth sinusoidal function, as shown in Fig. 16. The fifth harmonic in FES can then be reduced independently without any effect upon the other harmonics.

## VII. CONCLUSION

This paper addresses the effects of wobble disturbances on the optical disk drive. A comparison of AFC and FACT periodic cancellation methods on the wobble compensation has been described. Analysis and experimental results show that the AFC methods are not suitable for the cases where the DC content in periodic errors is insignificant with respect to other harmonics or is intended to be minimized. Contrast to AFC, the FACT controller is capable of compensating the DC content and undesired harmonics independently. Successful reduction in the harmonic components and DC content verifies that the FACT is promising in the application of industrial ODD systems, especially for disk runout and wobble compensation.

## REFERENCES

- [1] M. Bodson, A. Sacks, and P. Khosla, "Harmonic generation in adaptive feedforward cancellation schemes," *IEEE trans on Magnetics*, vol. 39, no. 9, pp. 1939–1944, 1994.
- [2] Y. Onuki, H. Ishioka, and H. Yada, "Repeatable runout compensation for disk drives using multi-loop adaptive feedforward cancellation," in *Proceedings of the SICE Annual Conference*, Chiba, 1998, pp. 1093–1098.
- [3] H. S. Lee, "Implementation of adaptive feedforward cancellation algorithm for pre-embossed rigid magnetic (perm) disks," *IEEE trans on Magnetics*, vol. 33, no. 3, pp. 2419–2423, 1997.
- [4] M. B. Alexei H. Sacks and W. Messner, "Advanced methods for repeatable runout compensation," *IEEE trans on Magnetics*, vol. 31, no. 2, pp. 1031–1036, 1995.
- [5] A. Sacks, M. Bodson, and P. Khosla, "Experimental results of adaptive periodic disturbance cancellation in a high performance magnetic disk drive," *Transactions of the ASME*, vol. 118, pp. 416–424, 1996.
- [6] W. Messner and M. Bodson, "Design of adaptive feedforward algorithms using internal model equivalence," *Internal Journal of Adaptive Control and Signal Processing*, vol. 9, pp. 199–212, 1995.
- [7] J. J. Liu and Y. P. Yang, "Frequency adaptive control technique for rejecting periodic runout," *Control Engineering Practice*, vol. 12, pp. 31–40, 2004.
- [8] J. J. Liu and Y. P. Yang, "Stability of the frequency adaptive control technique and its application to compact disk drives," *Control Engineering Practice*, On-line corrected proof: <http://dx.doi.org/10.1016/j.conengprac.2004.05.003>
- [9] D. S. Bayard, "Necessary and sufficient conditions for LTI representations of adaptive systems with sinusoidal regressors," in *Proceedings of the American Control Conference*, New Mexico, 1997, pp. 1642–1646.
- [10] B. A. Francis and W. M. Wonham, "The internal model principle of control theory," *Automatica*, vol. 12, pp. 457–465, 1976.
- [11] A. Hund, *Frequency Modulation*. McGraw-Hill Inc., 1942, first Edition.
- [12] S. Weerasooriya, J. L. Zhang, and T. S. Low, "Efficient implementation of adaptive feedforward runout cancellation in a disk drive," *IEEE trans. on Magnetics*, vol. 32, no. 5, pp. 3920–3923, 1996.
- [13] TEAC Test CD MCD-151A, TEAC Corporation, 2003, web site: <http://www.teac.co.jp>.